Efficient, numerically stable multiband $k\cdot p$ treatment of quantum transport in semiconductor heterostructures

Y. X. Liu,* D. Z.-Y. Ting,† and T. C. McGill
Thomas J. Watson Sr. Laboratory of Applied Physics, California Institute of Technology, Pasadena, California 91125
(Received 28 March 1996)

We present a method for treating quantum transport in heterostructures using multiband $\boldsymbol{k}\cdot\boldsymbol{p}$ theory. The method is similar to the multiband quantum transmitting boundary method developed earlier for use with multiband tight-binding band structure models, being efficient, numerically stable, and easy to implement. It also has the advantages of being intuitive to use and easy to generalize to include magnetic field and strain effects. We have applied this method to hole tunneling in prototypical *p*-type GaAs/AlAs double-barrier structure. [S0163-1829(96)05331-3]

I. INTRODUCTION

The physics of tunneling phenomena in semiconductor heterostructures has been a subject of considerable investigation since the early work of Tsu and Esaki.[1] A number of theoretical works have been developed for understanding and simulating the behavior of tunneling structures. The transfer-matrix method based on the original technique of Kane's $\boldsymbol{k}\cdot\boldsymbol{p}$ model[2] has been the most widely used. It is well known, however, that the transfer-matrix method, when used in conjunction with realistic multiband band-structure models, is numerically unstable for device structures larger than a few tens of Å.[3,4] To circumvent the numerical difficulties that arise in a transfer-matrix calculation, several techniques have been developed recently.[5–8] Among them, the multiband quantum transmitting boundary method (MQTBM) (Ref. 6) for tight-binding models has been shown to be equal to the transfer-matrix method in numerical efficiency, but superior in numerical stability and ease of implementation. The MQTBM is a multiband generalization of Frensley's[9] one-band effective-mass approximation implementation of the quantum transmitting boundary method, originally developed by Lent and Kirkner[10] for treating an electron wave guide using a finite-element approach. The tight-binding formulation of the MQTBM has been successfully implemented for the effective-bond-orbital model[11] to study interband tunneling in InAs/GaSb/AlSb systems,[6,12] and hole tunneling in GaAs/AlAs double-barrier heterostructures.[13] It has also been implemented in a Slater-Koster second-neighbor sp^3 tight-binding model[14] for studying X-point tunneling.[15] In this paper, we present the $\boldsymbol{k}\cdot\boldsymbol{p}$ version of the multiband quantum transmitting boundary method to complement the tight-binding MQTBM. Like the tight-binding version, MQTBM for $\boldsymbol{k}\cdot\boldsymbol{p}$ is numerically efficient and stable, and easy to implement. In addition, the $\boldsymbol{k}\cdot\boldsymbol{p}$ MQTBM has the following salient features: (1) $\boldsymbol{k}\cdot\boldsymbol{p}$ is readily familiar to many researchers, and, (2) it can be easily generalized to include magnetic-field and strain effects.

In Sec. II, we give a detailed account of the method we developed to study the tunneling phenomena in heterostructures. In Sec. III, we illustrate the method by applying it to the hole tunneling phenomena in a *p*-type GaAs/AlAs double-barrier structure, and briefly compare our method with some other available methods and also indicate how this method can be generalized for studying strain and magnetic-field effects. Finally, a summary is given in Sec. IV.

II. METHODS

The basic results of the effective-mass theory are that if the external potential V varies slowly over the unit cell, the effect of the periodic field of lattice can be replaced by a set of parameters H_{ij}, which are determined by the unperturbed bulk band structure. The solutions to the original Schrödinger's equation can be obtained by solving the following coupled differential equations:[16]

$$\sum_{j=1}^{M} [H_{ij}(-i\nabla)+V(\boldsymbol{r})]F_j = EF_i, \tag{1}$$

where the envelope functions F_i is related to the wave function by

$$\psi=\sum_{j=1}^{M} F_j u_{j0}, \tag{2}$$

where M is the number of the bands involved in the model, u_{i0} is the Bloch basis with lattice periodicity, and the form of matrix elements $H_{ij}(\boldsymbol{k})$ are determined by the $\boldsymbol{k}\cdot\boldsymbol{p}$ method.[2] In this paper, we will focus on one-dimensional quantum transport in semiconductor heterostructures in which the system varies only along the growth direction (x axis), and is translational invariant in the lateral directions. The key to our method is the treatment of boundary conditions, as developed originally by Lent and Kirkner.[10] Since this is much more easily explained in terms of a single-band model, for the sake of clarity we first give a brief summary of the technique developed by Frensley.[9] Then we generalize the method to the multiband in the $\boldsymbol{k}\cdot\boldsymbol{p}$ theory.

A. One-band model

In a simple one-band model with a parabolic band structure of effective mass m^*, the effective mass equation of the Hamiltonian is

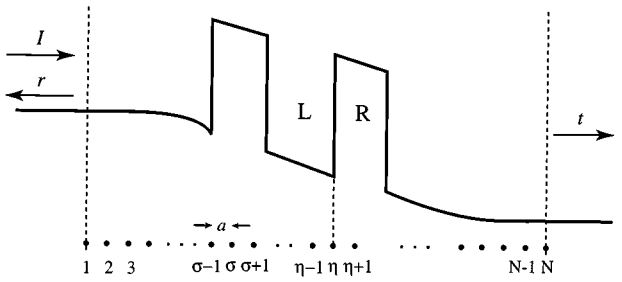

FIG. 1. The entire active device region is specified by N lattice points, typically with equal spacing a. The two boundaries are extended to flatband regions where electron states are plane-wave-like. The $\mathbf{k}\cdot\mathbf{p}$ differential equations are solved by applying the finite difference method to these lattice points.

$$-\frac{\hbar^2}{2}\frac{d}{dx}\left(\frac{1}{m^*}\frac{dF(x)}{dx}\right)+V(x)F(x)=EF(x). \tag{3}$$

At the heterointerface between two materials, the wave function and current continuity require that F and $(1/m^*)(dF/dx)$ be continuous across the interface.

In quantum tunneling problems, the boundary conditions are such that we have a known incoming plane-wave state from the left region, no incoming states from the right, and unknown outgoing transmitted and reflected plane-wave states in the right and left regions, respectively. The wave functions on the left and right flatband regions are expressed as

$$F_L=Ie^{ik_Lx}+re^{-ik_Lx}, \tag{4a}$$

$$F_R=te^{ik_Rx}, \tag{4b}$$

where I represents the known incoming plane-wave state from the left region, while t and r describe the transmitted and reflected states. The central issue in the quantum tunneling calculation is to evaluate the transmission coefficient t.

As schematically illustrated in Fig. 1, the entire device region is discretized into N lattice points $\{x_\sigma\}$, $\sigma=1,2,\ldots,N$, typically with equal spacing a. The two boundaries at the ends are extended to flatband regions where the electron states are plane-wave-like. If we choose a to be on the order of lattice spacing, within the framework of effective-mass theory, the derivatives of envelope function can then be well approximated by finite differences

$$\left.\frac{dF}{dx}\right|_{x_\sigma}\Rightarrow\frac{F_{\sigma+1}-F_\sigma}{a}, \tag{5a}$$

$$\left.\frac{d^2F}{dx^2}\right|_{x_\sigma}\Rightarrow\frac{F_{\sigma+1}+F_{\sigma-1}-2F_\sigma}{a^2}. \tag{5b}$$

To solve Schrödinger's Eq. (3) using the finite difference method, we carry the discretization in two steps: (1) Within each heterojunction layer, the effective mass m^* is assumed to be constant, and the external potential varies slowly within lattice spacing. (2) At the heterointerface, we assume the current density is constant.

In each heterostructure region, Schrödinger's Eq. (3) can be discretized as

$$-\frac{\hbar^2}{2m^*a^2}F_{\sigma-1}+\left(\frac{\hbar^2}{m^*a^2}+V(x_\sigma)-E\right)F_\sigma-\frac{\hbar^2}{2m^*a^2}F_{\sigma+1}=0, \tag{6}$$

and similarly at each heterointerface $\sigma=\eta$, the current continuity condition $(1/m^*)(dF/dx)$ can be discretized as

$$-\frac{1}{m_L^*}F_{\eta-1}+\left(\frac{1}{m_L^*}+\frac{1}{m_R^*}\right)F_\eta-\frac{1}{m_R^*}F_{\eta+1}=0, \tag{7}$$

where L and R label the left and right regions of the heterointerface. Equations (6) and (7) can all be written in the form

$$H_{\sigma,\sigma-1}F_{\sigma-1}+H_{\sigma,\sigma}F_\sigma+H_{\sigma,\sigma+1}F_{\sigma+1}=0,\quad \sigma=2,\ldots,N-1. \tag{8}$$

These constitute a set of linear equations on the discretized envelope functions F_σ.

The key idea in Frensley's treatment of boundary conditions is to eliminate the unknown r and t from Eq. (4) and formulate the problem as a system of linear equations with only the envelope functions as the unknowns. At $\sigma=1$ and 2, Eq. (4a) gives

$$F_1=I+r, \tag{9a}$$

$$F_2=Ie^{ik_La}+re^{-ik_La}. \tag{9b}$$

Eliminating r, we obtain

$$F_1-e^{ik_La}F_2=I(1-e^{i2k_La}). \tag{10}$$

Similarly applying the technique to the boundary condition at the right region, Eq. (4b), we have

$$F_{N-1}e^{ik_Ra}-F_N=0. \tag{11}$$

The above equations, together with Eq. (8), constitute a system of N linear equations which can be written in matrix form as

$$\begin{bmatrix} 1 & -e^{ik_La} & 0 & \cdots & \cdots & \cdots & 0 \\ H_{2,1} & H_{2,2} & H_{2,3} & 0 & \cdots & \cdots & 0 \\ 0 & H_{3,2} & H_{3,3} & H_{3,4} & 0 & \cdots & 0 \\ \vdots & & \ddots & \ddots & \ddots & \vdots & \vdots \\ 0 & & & 0 & H_{N-1,N-2} & H_{N-1,N-1} & H_{N-1,N} \\ 0 & \cdots & \cdots & \cdots & 0 & -e^{ik_Ra} & 1 \end{bmatrix}\begin{bmatrix} F_1 \\ F_2 \\ F_3 \\ \vdots \\ F_{N-1} \\ F_N \end{bmatrix}=\begin{bmatrix} I(1-e^{i2k_Ra}) \\ 0 \\ 0 \\ \vdots \\ 0 \\ 0 \end{bmatrix}. \tag{12}$$

The boundary conditions of incoming and outgoing plane-wave states in quantum tunneling problems are represented by the boundary and inhomogeneous terms in this system of linear equations.

Equation (12) can be solved readily using standard numerical mathematical algorithms. Having obtained the coefficients of envelope function F_i, it follows from Eq. (4b) that the coefficient of transmitted plane-wave states t is given by

$$t = e^{-ik_R(N-1)a} F_N . \tag{13}$$

The transmission coefficient is given by the ratio of transmitted and incident probability current densities (given by plane-wave absolute square amplitude times group velocity, which, in turn, is proportional to the k gradient of the band structure),

$$T(E) = \frac{S_t}{S_I} = \frac{|t|^2 |v_R|}{|I|^2 |v_L|} = \frac{|t|^2}{|I|^2} \frac{|\nabla_k E_R|}{|\nabla_k E_L|}. \tag{14}$$

$E_L(k)$ and $E_R(k)$ are the energy dispersions of the incident and the transmitted bulk plane-wave states, respectively, which can be obtained by solving Eq. (3) in the left and right flatband regions.

B. General multiband model

1. Discretization of Schrödinger's equation

It is quite straightforward to generalize the method illustrated in the one-band model to multiband cases. The effective-mass equations in multiband models are described by a set of coupled differential equation of envelope functions,[16]

$$\sum_{j=1}^{M} [H_{ij}(-i\nabla) + V(\boldsymbol{r})] F_j = E F_i , \tag{15}$$

where M is the number of bands in the model. The bulk band matrix element H_{ij} in the second-order $\mathbf{k}\cdot\mathbf{p}$ method, can be generally written as

$$H_{ij} = D_{ij}^{(2)\alpha\beta} k_\alpha k_\beta + D_{ij}^{(1)\alpha} k_\alpha + D_{ij}^{(0)} \tag{16}$$

where indices α and β are summed over x, y, and z. The linear terms in k usually appear when the model includes explicitly the interaction between conduction band and valence bands of the system.

The problems we consider are one dimensional, in which the system varies only along the growth direction (x axis), and is translational invariant in the lateral directions. We can rewrite the the Hamiltonian matrix element, Eq. (16) as a second-order polynomial in k_x,

$$H_{ij} = H_{ij}^{(2)} k_x^2 + H_{ij}^{(1)}(\boldsymbol{k}_\parallel) k_x + H_{ij}^{(0)}(\boldsymbol{k}_\parallel), \tag{17}$$

with $\boldsymbol{k}_\parallel = k_y \hat{y} + k_z \hat{z}$. In short, we can write

$$\boldsymbol{H}(\boldsymbol{k}) = \boldsymbol{H}^{(2)} k_x^2 + \boldsymbol{H}^{(1)}(\boldsymbol{k}_\parallel) k_x + \boldsymbol{H}^{(0)}(\boldsymbol{k}_\parallel) \tag{18}$$

where $\boldsymbol{H}^{(n)}$ are $M \times M$ matrices. An example of decomposing the $\mathbf{k}\cdot\mathbf{p}$ Hamiltonian matrix element for the Γ_8 4×4 valence band states is given in the Appendix.

Similar to the treatment in Sec. II A, the discretization of Schrödinger's equation [Eq. (15)] is carried out in two steps: (1) Within each heterostructure layer, the Luttinger parameters are assumed to be constants. (2) At the heterointerface, the current density is assumed to be constant across the interface.

Within each heterostructure layer, replacing k_x with the operator $(1/i)(\partial/\partial x)$, Eq. (15) becomes

$$\left(-\boldsymbol{H}^{(2)} \frac{\partial^2}{\partial x^2} - i\boldsymbol{H}^{(1)} \frac{\partial}{\partial x} + \boldsymbol{H}^{(0)} + V(x) \right) \boldsymbol{F} = E\boldsymbol{F}. \tag{19}$$

Where $\boldsymbol{F}$ is a vector of length M. Applying the finite difference approximations of Eq. (5) at each discretized lattice point σ, the M coupled differential equations (19) are then transformed into M linear finite difference equations,

$$\boldsymbol{H}_{\sigma,\sigma+1}\boldsymbol{F}_{\sigma+1} + \boldsymbol{H}_{\sigma,\sigma}\boldsymbol{F}_{\sigma} + \boldsymbol{H}_{\sigma,\sigma-1}\boldsymbol{F}_{\sigma-1} = 0, \tag{20}$$

with

$$\boldsymbol{H}_{\sigma,\sigma} = \frac{2\boldsymbol{H}^{(2)}}{a^2} + \boldsymbol{H}^{(0)} + V_\sigma - E, \tag{21a}$$

$$\boldsymbol{H}_{\sigma,\sigma+1} = -\frac{\boldsymbol{H}^{(2)}}{a^2} - i\frac{\boldsymbol{H}^{(1)}}{2a}, \tag{21b}$$

$$\boldsymbol{H}_{\sigma,\sigma-1} = -\frac{H^{(2)}}{a^2} + i\frac{\boldsymbol{H}^{(1)}}{2a}, \tag{21c}$$

where $\boldsymbol{H}_{\sigma,\sigma'}$ are $M\times M$ matrices. Equation (20) has a form similar to the tight-binding formulation with nearest-neighbor interaction. This important observation led us to develop a similar method, based on the multiband $\mathbf{k}\cdot\mathbf{p}$ theory, to that of the tight-binding MQTBM approach for treating quantum transport.

2. Current-density operator

It can be shown that the probability current density operator in the $\mathbf{k}\cdot\mathbf{p}$ theory is then given by[4,17]

$$J_x = \frac{1}{i\hbar}\left(\boldsymbol{F}^\dagger \boldsymbol{H}^{(2)} \frac{\partial \boldsymbol{F}}{\partial x} - \frac{\partial \boldsymbol{F}^\dagger}{\partial x}\boldsymbol{H}^{(2)}\boldsymbol{F} + i\boldsymbol{F}^\dagger \boldsymbol{H}^{(1)} \boldsymbol{F} \right)$$

$$= \mathrm{Re}(\boldsymbol{F}^\dagger \boldsymbol{J}_x \boldsymbol{F}), \tag{22}$$

with

$$\boldsymbol{J}_x = \frac{1}{\hbar}\left(-2i\boldsymbol{H}^{(2)} \frac{\partial}{\partial x} + \boldsymbol{H}^{(1)} \right). \tag{23}$$

3. Treatment of heterostructure interfaces

At the heterojunction interface $\sigma = \eta$, the wave function and current are required to be continuous across the interface. Following the treatment of Altarelli,[18] we ignore the differences in the Bloch basis functions u_{i0} for materials across the heterointerface. Then the condition of wave function continuity results in the continuity of envelope functions

$$\boldsymbol{F}_L = \boldsymbol{F}_R . \tag{24}$$

The current continuity requires that $\boldsymbol{J}_x\boldsymbol{F}$ or

$$-2i\boldsymbol{H}^{(2)}\frac{\partial \boldsymbol{F}}{\partial x}+\boldsymbol{H}^{(1)}\boldsymbol{F} \tag{25}$$

be continuous across the interface. So the $\boldsymbol{H}$ matrices at the interface should be corrected as

$$\boldsymbol{H}_{\eta,\eta}=\frac{2(\boldsymbol{H}_R^{(2)}+\boldsymbol{H}_L^{(2)})}{a^2}-i\frac{\boldsymbol{H}_R^{(1)}-\boldsymbol{H}_L^{(1)}}{2a}, \tag{26a}$$

$$\boldsymbol{H}_{\eta,\eta+1}=-\frac{2\boldsymbol{H}_R^{(2)}}{a^2}-i\frac{\boldsymbol{H}_R^{(1)}}{2a}, \tag{26b}$$

$$\boldsymbol{H}_{\eta,\eta-1}=-\frac{2\mathbf{H}_L^{(2)}}{a^2}+i\frac{\mathbf{H}_L^{(1)}}{2a}. \tag{26c}$$

4. Boundary conditions

In calculating the transmission coefficient in tunneling problems, accurate treatment of the boundary condition is crucial. The formulation of boundary conditions in the multiband model is more sophisticated, and deserves special attention. In bulk flatband region, the Bloch plane-wave solutions of wave vector $\boldsymbol{k}$ can be generally written as

$$\boldsymbol{F}_{\boldsymbol{k}}=e^{i\mathbf{k}\cdot\mathbf{r}}\boldsymbol{C}_{\boldsymbol{k}}, \tag{27}$$

where $\boldsymbol{C}_{\boldsymbol{k}}$ satisfies that

$$\boldsymbol{H}(\boldsymbol{k})\boldsymbol{C}_{\boldsymbol{k}}=E\boldsymbol{C}_{\boldsymbol{k}}. \tag{28}$$

Matrix elements $H_{ij}(\boldsymbol{k})$ are generally a quadratic polynomial in k_α, so for fixed energy E and in-plane wave vector $\boldsymbol{k}_\parallel$ there will be $2M$ complex wave vector solutions $k_{x,j}$ and associated eigenstates $\boldsymbol{C}_{\boldsymbol{k}_j}$ in general. The wave function ψ for given energy E is in general a linear combination of these solutions,

$$\boldsymbol{F}(\boldsymbol{r})=e^{i\mathbf{k}_\parallel\cdot\mathbf{r}_\parallel}\sum_{j=1}^{2M} b_i e^{ik_{x,j}x}\boldsymbol{C}_{\boldsymbol{k}_j}, \tag{29}$$

$$\psi=\boldsymbol{F}(\boldsymbol{r})\boldsymbol{u}_0(\boldsymbol{r}). \tag{30}$$

To find the $2M$ eigenstates given the energy E and $\mathbf{k}_\parallel$, we rewrite Eq. (28) explicitly using Eq. (18) as

$$[\boldsymbol{H}^{(2)}k_x^2+\boldsymbol{H}^{(1)}(\boldsymbol{k}_\parallel)k_x+\boldsymbol{H}^{(0)}(\boldsymbol{k}_\parallel)-E]\boldsymbol{C}_{\boldsymbol{k}}=0 \tag{31}$$

The generalized eigenvalue problem of Eq. (31) can be converted into the standard eigenvalue form for k_x,[19,20]

$$\begin{bmatrix} 0 & 1 \\ -(\boldsymbol{H}^{(2)})^{-1}[\boldsymbol{H}^{(0)}(\boldsymbol{k}_\parallel)-E] & -(\boldsymbol{H}^{(2)})^{-1}\boldsymbol{H}^{(1)}(\boldsymbol{k}_\parallel) \end{bmatrix}\begin{bmatrix} \mathbf{C}_{\mathbf{k}} \\ k_x\boldsymbol{C}_{\boldsymbol{k}} \end{bmatrix} = k_x\begin{bmatrix} \boldsymbol{C}_{\boldsymbol{k}} \\ k_x\boldsymbol{C}_{\boldsymbol{k}} \end{bmatrix}. \tag{32}$$

It can be shown that the matrix $\mathbf{H}^{(2)}$ is nonsingular.[3] Equation (32) has $2M$ eigenvalues $k_{x,j}$ solutions and $2M$ corresponding eigenvectors $\boldsymbol{C}_{\boldsymbol{k},j}$. This method is much more convenient and efficient than some other calculations of the complex band structures,[4,21] which involves finding the zeros of the secular determinant $\det[\boldsymbol{H}(\boldsymbol{k})-E]$.

The boundary conditions are such that the wave function in the left region includes both the incoming and reflected plane-wave states, and the wave function on the right region has only transmitted plane-wave states. The eigenvalues $k_{x,j}$ in general can be complex values describing evanescent states. Following the treatment of boundary conditions by Ting, Yu, and McGill,[6] we order the wave vectors $k_{x,j}$ such that $j=1,2,\ldots,M$ corresponds to the forward states which propagate or decay to the right (i.e., $k_{x,j}$ is either positive real number or its imaginary part is positive for electron states, and vice versa for hole states), while $j=M+1,\ldots,2M$ corresponds to the backward states which propagate or decay to the left. The boundary conditions can be described in the bulk eigenstate basis by choosing the proper form for the wave functions in the left and right regions:

$$\boldsymbol{F}_L=\exp(i\mathbf{k}_\parallel\cdot\mathbf{r}_\parallel)\sum_{j=1}^{M}(I_j e^{ik_{x,j}^L x}\boldsymbol{C}_{\boldsymbol{k},j}+r_j e^{ik_{x,j+M}^L x}\boldsymbol{C}_{\boldsymbol{k}_L,j+M}), \tag{33a}$$

$$\boldsymbol{F}_R=\exp(i\mathbf{k}_\parallel\cdot\mathbf{r}_\parallel)\sum_{j=1}^{M} t_j e^{ik_{x,j}^R x}\boldsymbol{C}_{\boldsymbol{k}_R,j}. \tag{33b}$$

where $k_{x,j}^L$ and $k_{x,j}^R$ are the bulk complex wave vectors in the left and right regions, respectively. In bulk crystals, the number of states propagating to the right should equal the number of states propagating to the left. Similarly, the number of states decaying to the right should equal to the number of states decaying to the left.

Let $\boldsymbol{I}$, $\boldsymbol{r}$, and $\boldsymbol{t}$ be column vectors of dimension M containing the coefficients $\{I_j\}$, $\{r_j\}$, and $\{t_j\}$, respectively. $\boldsymbol{I}$ represents the known incoming states, while $\boldsymbol{r}$ and $\boldsymbol{t}$ describe the reflected and transmitted components. By examining Eqs. (33a) and (33b), we find that $\boldsymbol{I}$, $\boldsymbol{r}$, and $\boldsymbol{t}$ are related to the envelope-function coefficients by a simple basis transformation,

$$\begin{bmatrix} \boldsymbol{F}_1 \\ \boldsymbol{F}_2 \end{bmatrix}=\begin{bmatrix} \boldsymbol{D}_{11}^L & \boldsymbol{D}_{12}^L \\ \boldsymbol{D}_{21}^L & \boldsymbol{D}_{22}^L \end{bmatrix}\begin{bmatrix} \boldsymbol{I} \\ \boldsymbol{r} \end{bmatrix}, \tag{34a}$$

$$\begin{bmatrix} \mathbf{F}_{N-1} \\ \mathbf{F}_N \end{bmatrix}=\begin{bmatrix} \mathbf{D}_{11}^R & \mathbf{D}_{12}^R \\ \mathbf{D}_{21}^R & \mathbf{D}_{22}^R \end{bmatrix}\begin{bmatrix} \mathbf{t} \\ 0 \end{bmatrix}. \tag{34b}$$

where $\boldsymbol{D}_{11}^L$, $\boldsymbol{D}_{12}^L$ and $\boldsymbol{D}_{11}^R$, $\boldsymbol{D}_{12}^R$ are $M\times M$ matrices whose column vectors are the eigenvectors $\boldsymbol{C}_{\boldsymbol{k}_L,j}$ and $\boldsymbol{C}_{\boldsymbol{k}_R,j}$ obtained by solving Eq. (32) for the left and right regions, respectively, and arranged in the same order as the corresponding eigenvalues:

$$\boldsymbol{D}_{11}^{\lambda}=[\boldsymbol{C}_{\boldsymbol{k}_\lambda,1},\ \boldsymbol{C}_{\boldsymbol{k}_\lambda,2},\ \ldots,\ \boldsymbol{C}_{\boldsymbol{k}_\lambda,M}], \tag{35a}$$

$$\boldsymbol{D}_{12}^{\lambda}=[\boldsymbol{C}_{\boldsymbol{k}_\lambda,M+1},\ \boldsymbol{C}_{\boldsymbol{k}_\lambda,M+2},\ \ldots,\ \boldsymbol{C}_{\boldsymbol{k}_\lambda,2M}], \tag{35b}$$

and

$$\boldsymbol{D}_{21}^{\lambda}=[e^{ik_{x,1}^{\lambda}a}\boldsymbol{C}_{\boldsymbol{k}_{\lambda},1},\ e^{ik_{x,2}^{\lambda}a}\boldsymbol{C}_{\boldsymbol{k}_{\lambda},2},\ \ldots,\ e^{ik_{x,M}^{\lambda}a}\boldsymbol{C}_{\boldsymbol{k}_{\lambda},M}], \tag{36a}$$

$$\boldsymbol{D}_{21}^{\lambda}=[e^{ik_{x,M+1}^{\lambda}a}\boldsymbol{C}_{\boldsymbol{k}_{\lambda},M+1},\ e^{ik_{x,M+2}^{\lambda}a}\boldsymbol{C}_{\boldsymbol{k}_{\lambda},M+2},\ \ldots,\ e^{ik_{x,2M}^{\lambda}a}\boldsymbol{C}_{\boldsymbol{k}_{\lambda},2M}], \tag{36b}$$

where $\lambda=L$ and R.

Now pursuing the same technique we applied in the one-band model, we eliminate **r** and **t** from Eqs. (34a) and (34a),

$$\boldsymbol{F}_1-\boldsymbol{D}_{12}^{L}\boldsymbol{D}_{22}^{L\,-1}\boldsymbol{F}_2=\boldsymbol{D}_{11}^{L}\boldsymbol{I}-\boldsymbol{D}_{12}^{L}\boldsymbol{D}_{22}^{L\,-1}\boldsymbol{D}_{21}^{L}\boldsymbol{I}, \tag{37a}$$

$$-\boldsymbol{D}_{21}^{R}\boldsymbol{D}_{11}^{R\,-1}\boldsymbol{F}_{N-1}+\boldsymbol{F}_N=\boldsymbol{0}. \tag{37b}$$

which are the generalized multiband forms of Eqs. (10) and (11). These equations, together with Eq. (20), constitute a system of MN linear equations. This can be written in the following matrix form corresponding to the generalized multiband model:

$$\begin{bmatrix} \boldsymbol{1} & -\boldsymbol{D}_{12}^{L}\boldsymbol{D}_{22}^{L\,-1} & \boldsymbol{0} & \cdots & \cdots & \cdots & \boldsymbol{0} \\ \boldsymbol{H}_{2,1} & \boldsymbol{H}_{2,2} & \boldsymbol{H}_{2,3} & \boldsymbol{0} & \cdots & \cdots & \boldsymbol{0} \\ \boldsymbol{0} & \boldsymbol{H}_{3,2} & \boldsymbol{H}_{3,3} & \boldsymbol{H}_{3,4} & \boldsymbol{0} & \cdots & \boldsymbol{0} \\ \vdots & & \ddots & \ddots & \ddots & \vdots & \\ \boldsymbol{0} & & & \boldsymbol{0} & \boldsymbol{H}_{N-1,N-2} & \boldsymbol{H}_{N-1,N-1} & \boldsymbol{H}_{N-1,N} \\ \boldsymbol{0} & \cdots & \cdots & \cdots & \boldsymbol{0} & -\boldsymbol{D}_{21}^{R}\boldsymbol{D}_{11}^{R\,-1} & \boldsymbol{1} \end{bmatrix} \cdot \begin{bmatrix} \boldsymbol{F}_1 \\ \boldsymbol{F}_2 \\ \boldsymbol{F}_3 \\ \vdots \\ \boldsymbol{F}_{N-1} \\ \boldsymbol{F}_N \end{bmatrix} = \begin{bmatrix} \boldsymbol{D}_{11}^{L}\boldsymbol{I}-\boldsymbol{D}_{12}^{L}\boldsymbol{D}_{22}^{L\,-1}\boldsymbol{D}_{21}^{L}\boldsymbol{I} \\ \boldsymbol{0} \\ \boldsymbol{0} \\ \vdots \\ \boldsymbol{0} \\ \boldsymbol{0} \end{bmatrix} \tag{38}$$

Having obtained the envelope function coefficients $\mathbf{F}_{\sigma}$, it follows from Eq. (34b) that the coefficients of the transmitted plane-wave states are given by

$$\boldsymbol{t}=\boldsymbol{D}_{21}^{R\,-1}\boldsymbol{F}_N. \tag{39}$$

Taking the normalization condition of $|I|=1$, the total transmission coefficient can be calculated from Eq. (22):[21]

$$T(E,k_{\parallel})=\sum_{j=1}^{M}|t_j(E,k_{\parallel})|^2\frac{\mathrm{Re}(\boldsymbol{C}_j^{\dagger}\boldsymbol{J}_x\boldsymbol{C}_j)}{\mathrm{Re}(\boldsymbol{C}_I^{\dagger}\boldsymbol{J}_x\boldsymbol{C}_I)}. \tag{40}$$

It can be shown[4] that the current components for a given subband $\boldsymbol{j}_j=\mathrm{Re}(\boldsymbol{C}_j^{\dagger}\hat{\boldsymbol{J}}\boldsymbol{C}_j)$ is related to the group velocity $\boldsymbol{v}_j=(1/\hbar)\nabla_{\boldsymbol{k}}E_j(\boldsymbol{k})$ by

$$\boldsymbol{j}=\rho\boldsymbol{v}, \tag{41}$$

where $\rho=\boldsymbol{C}^{\dagger}\boldsymbol{C}$. So the transmission coefficient T can also be expressed as

$$T(E,k_{\parallel})=\sum_{j=1}^{M}|t_j(E,k_{\parallel})|^2\frac{|v_j(E,k_{\parallel};R)|}{|v_I(E,k_{\parallel};L)|}. \tag{42}$$

III. APPLICATIONS AND DISCUSSIONS

A. *p*-type GaAs/AlAs double barrier

For the purpose of illustration of our method, we consider the top of valence-band Γ_8 states. The four basis functions and the 4×4 Luttinger-Kohn Hamiltonian are given explicitly in the Appendix. The lack of inversion symmetry in the III-V system is not represented by this Hamiltonian, therefore the bands have a twofold degeneracy at every point in k space. It is known that states $KJ\psi_{\mathbf{k},\uparrow}=\psi_{\mathbf{k},\downarrow}$ and $\psi_{\mathbf{k},\uparrow}$ are degenerate in energy and are orthogonal to each other,[22] where K is the Kramers time reversal operator and J is the space inversion operator.

Due to the degeneracy, the electron eigenstates $\boldsymbol{C}_k$ for a given energy E and k are not uniquely determined. For $\boldsymbol{k}_{\parallel}=0$, the eigenstates are decoupled into spin-up and spin-down pure heavy-hole and light-hole states. In the case of $\boldsymbol{k}_{\parallel}\neq0$, there is mixing between heavy-hole and light-hole bases. We construct and label the electron eigenstate basis in the following convention. The two degenerate basis for a given energy E and k are constructed to be $\psi_{\boldsymbol{k},\uparrow}$ and $KJ\psi_{\boldsymbol{k},\uparrow}$. For heavy-hole bands, $\psi_{\boldsymbol{k}_{\mathrm{hh}},\uparrow}$ is constructed so that the heavy hole component with spin-down is zero,

$$\boldsymbol{C}_{k_{\mathrm{HH}},\uparrow}=(u_1,u_2,u_3,0).$$

Its degenerate counterpart is therefore given by

$$\boldsymbol{C}_{k_{\mathrm{HH}},\downarrow}=(0,u_3^{*},-u_2^{*},u_1^{*}),$$

in which the spin-up heavy-hole (HH) component vanishes. Similarly, for light-hole (LH) bands, we choose

$$\boldsymbol{C}_{k_{\mathrm{LH}},\uparrow}=(v_1,v_2,0,v_4),$$

and

$$\boldsymbol{C}_{k_{\mathrm{LH}},\downarrow}=(-v_4^{*},0,-v_2^{*},v_1^{*}).$$

These four eigenstates are orthogonal to each other and constitute the basis for the electron states in the Γ_8 valence band.

The GaAs/AlAs double-barrier resonant tunneling structure we consider has 50-Å well width and 30-Å barrier width. In our calculation, the flatband condition is assumed. By assumption of the effective-mass theory, the envelope functions vary slowly on the scale of the unit cell size, therefore it is a good approximation to take the lattice constant as the step size in our discretization.

Figure 2 shows the transmission coefficients for normal incident HH and LH states. In the case $\boldsymbol{k}_{\parallel}=0$, the HH and LH states are decoupled:

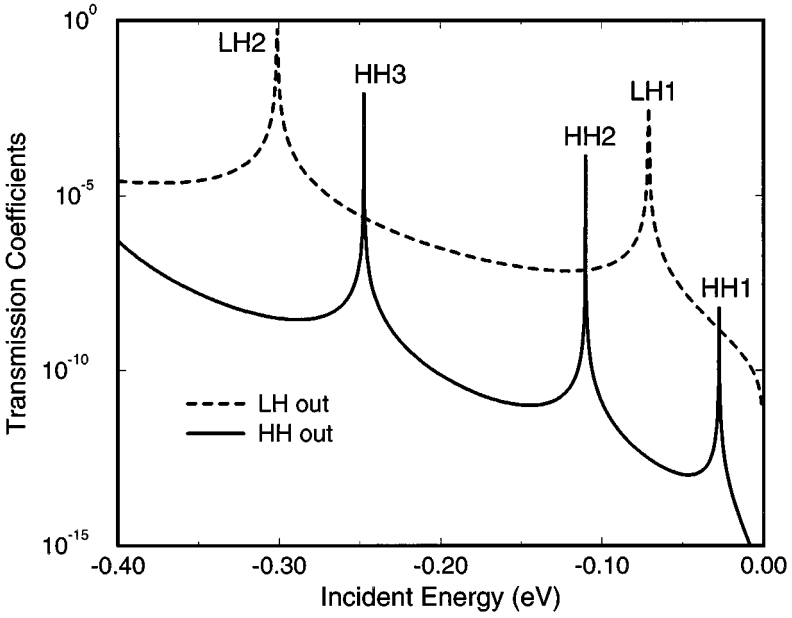

FIG. 2. Transmission coefficients for heavy-hole (solid line) and light-hole (dashed line) states through a 30 Å - 50 Å - 30 Å double-barrier heterostructure with $k_{\|}=0$.

$$\boldsymbol{H}^{(2)}=\frac{\hbar^2}{2m}\begin{bmatrix}\gamma_1-2\gamma_2 & 0 & 0 & 0\\ 0 & \gamma_1+2\gamma_2 & 0 & 0\\ 0 & 0 & \gamma_1+2\gamma_2 & 0\\ 0 & 0 & 0 & \gamma_1-2\gamma_2\end{bmatrix}, \tag{43a}$$

$$\boldsymbol{H}^{(1)}(\boldsymbol{k}_{\|})=\boldsymbol{H}^{(0)}(\boldsymbol{k}_{\|})=0. \tag{43b}$$

The results would be the same as the ones derived using simple one-band model, assuming the heavy-hole and light-hole effective masses are

$$m^*_{\mathrm{HH}}=\frac{m}{\gamma_1-2\gamma_2}, \tag{44a}$$

$$m^*_{\mathrm{LH}}=\frac{m}{\gamma_1+2\gamma_2}, \tag{44b}$$

respectively. The resonant peaks correspond to the quasi-bound HH and LH states in the central well. As expected, the light-hole state has a higher transmission coefficient than the heavy hole due to smaller effective mass.

In Figs. 3 and 4, respectively, we show the transmission coefficients for incoming HH and LH states with $|\boldsymbol{k}_{\|}|=0.03$ Å^{-1}. The nonzero $\boldsymbol{k}_{\|}$ states contain mixing of heavy- and light-hole states, and interact with all the quasibound states formed in the well, resulting in multiple transmission resonances. The resonant states are labeled according to their dominant bulk-state component. Because of the hole-mixing effects, the incident heavy-hole state can transmit through

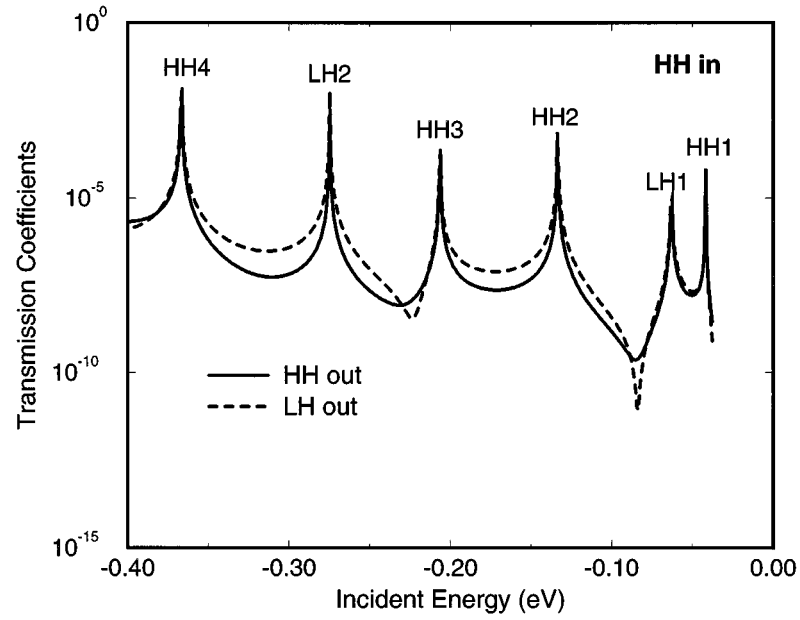

FIG. 3. Transmission coefficients for heavy-hole (solid line) and light-hole (dashed line) channels with a heavy-hole incoming state through a 30 Å - 50 Å - 30 Å double-barrier heterostructure with $k_{\|}=0.03$ Å^{-1}.

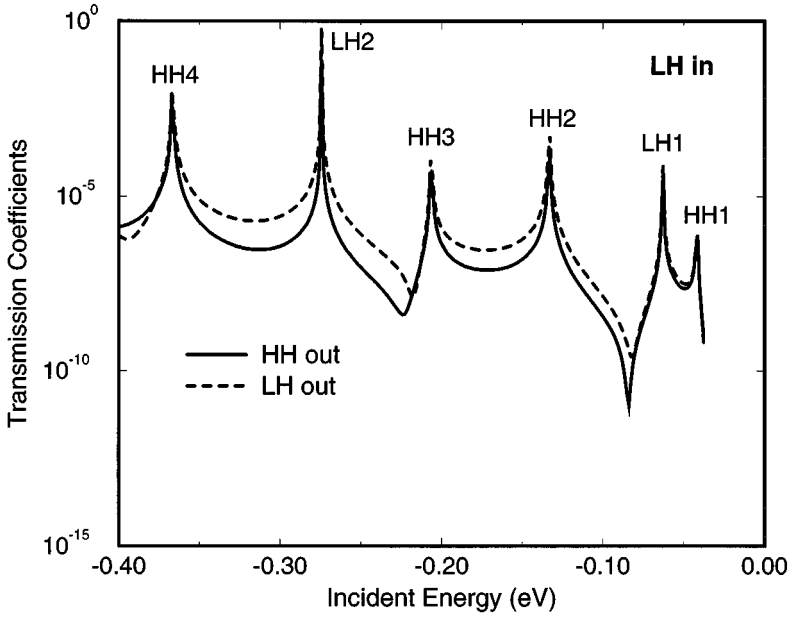

FIG. 4. Transmission coefficients for heavy-hole (solid line) and light-hole (dashed line) channels with a light-hole incoming state through a 30 Å - 50 Å - 30 Å double-barrier heterostructure with $k_{\|}=0.03$ Å $^{-1}$.

not only the heavy-hole channel, but also the light-hole channel, and vice versa for the incident light-hole state. This hole-mixing effects in p-type GaAs/AlAs double-barrier structures have been observed in experimental I-V characteristics.[23]

B. Discussions

We first briefly compare our method with some other available methods. The well-known transfer-matrix method has been employed for studying hole tunneling in the framework of $\boldsymbol{k}\cdot\boldsymbol{p}$ theory.[4,18,17] However, in addition to numerical instability problems occurred for devices larger than a few tens of Å,[3] spherical approximation had to be used to simplify the multiband plane-wave solutions at each piecewise-constant potential region. The computational cost for an efficient implementation of the transfer-matrix method is the same as our method.[6] Therefore, the method we presented here has a considerable advantage over the transfer-matrix method.

The scattering matrix method developed by Ko and Inkson[5] overcomes the numerical instability problem in transfer-matrix method by separating the forward and backward states, and relating the outgoing and incoming states through the scattering matrix. By doing so, the less localized and the propagating states dominate numerically, and the physics of tunneling process is more faithfully described. However, the gain in numerical stability is somewhat offset by added computational cost in constructing the scattering matrix, especially in localized orbital band-structure models.

The computational technique we developed here is similar to the MQTBM (Ref. 6) for tight-binding models, that is, it transforms the entire problem to a system of linear equations in the final form. They are both efficient, numerically stable and easy to implement. They complement each other in various applications. Problems like X-point tunneling are more easily studied under the tight-binding framework.[15] On the other hand, $\boldsymbol{k}\cdot\boldsymbol{p}$ method presented here has the advantages of being readily familiar to many researchers, and easy to extend to incorporate the strain and magnetic-field effects. The strain effect adds either a constant or linear term on the $\boldsymbol{k}\cdot\boldsymbol{p}$ matrix element,[24] and the magnetic field effect only affects the matrix element by transforming $\boldsymbol{k}\rightarrow\boldsymbol{k}-(e\boldsymbol{A}/c)$ and including the constant magnetic moment energy.[25] Since the matrix elements in Eq. (38) are constructed directly from the $\boldsymbol{k}\cdot\boldsymbol{p}$ matrix elements, it is very convenient to implement this method for various material systems. The application to the magnetotunneling effect in interband and intraband heterostructures will be published elsewhere.

IV. SUMMARY

We have developed a method for quantum transport calculation in semiconductor heterostructures. The method is based on the multiband $\boldsymbol{k}\cdot\boldsymbol{p}$ theory and the multiband quantum transmitting boundary method.[6] The method circumvents the numerical instability encountered in the transfer-matrix method, and is efficient and easy to implement. The formulation based on $\boldsymbol{k}\cdot\boldsymbol{p}$ theory makes it suitable for studying strain and magnetic-field effects. We have demonstrated the utility of the method by applying it to the hole tunneling in p-type GaAs/AlAs double-barrier structures.

ACKNOWLEDGMENTS

The authors would like to thank R. R. Marquardt for helpful discussions. This work is supported by the Office of Naval Research (ONR) under Grant No. N00014-89-J-1141.

APPENDIX A: BASIS AND HAMILTONIAN OF Γ_8 STATES

The basis functions for the top of the valence-band Γ_8 states are chosen to be

$$u_1=|\tfrac{3}{2},\tfrac{3}{2}\rangle=\left(\frac{X+iY}{\sqrt{2}}\right)\uparrow, \tag{A1a}$$

$$u_2=\left|\tfrac{3}{2},\tfrac{1}{2}\right\rangle=\frac{1}{\sqrt{6}}[(X+iY)\downarrow-2Z\uparrow], \tag{A1b}$$

$$u_3=\left|\tfrac{3}{2},-\tfrac{1}{2}\right\rangle=-\frac{1}{\sqrt{6}}[(X-iY)\uparrow+2Z\downarrow], \tag{A1c}$$

$$u_4=\left|\tfrac{3}{2},-\tfrac{3}{2}\right\rangle=-\left(\frac{X-iY}{\sqrt{2}}\right)\downarrow. \tag{A1d}$$

The phases of these basis satisfy $Cu_1=u_4$, $Cu_4=-u_1$, $Cu_2=-u_3$, and $Cu_3=u_2$, where the conjugation operator $C=JK$ is the product of space inversion operator J and the Kramers time reversal operator K.

The Luttinger-Kohn Hamiltonian is given by

$$\boldsymbol{H}(\boldsymbol{k})=\begin{bmatrix} P+Q & -S & R & 0 \\ -S^* & P-Q & 0 & R \\ R^* & 0 & P-Q & S \\ 0 & R^* & S^* & P+Q \end{bmatrix}, \tag{A2}$$

with

$$P(\boldsymbol{k})=\frac{\hbar^2}{2m}\gamma_1 k^2-E_V, \tag{A3a}$$

$$Q(\boldsymbol{k})=\frac{\hbar^2}{2m}\gamma_2(k_x^2+k_y^2-2k_z^2), \tag{A3b}$$

$$S(\boldsymbol{k})=\frac{\hbar^2}{2m}2\sqrt{3}\gamma_3(k_x-ik_y)k_z, \tag{A3c}$$

$$R(\boldsymbol{k})=\frac{\hbar^2}{2m}\sqrt{3}[-\gamma_2(k_x^2-k_y^2)+2i\gamma_3 k_x k_y]. \tag{A3d}$$

Choosing the growth direction along the z direction, $H(\boldsymbol{k})$ can be decomposed as

$$\boldsymbol{H}(\boldsymbol{k})=\boldsymbol{H}^{(2)}k_z^2+\boldsymbol{H}^{(1)}(\boldsymbol{k}_\parallel)k_z+\boldsymbol{H}^{(0)}(\mathbf{k}_\parallel) \tag{A4}$$

where

$$\boldsymbol{H}^{(2)}=\frac{\hbar^2}{2m}\begin{bmatrix} \gamma_1-2\gamma_2 & 0 & 0 & 0 \\ 0 & \gamma_1+2\gamma_2 & 0 & 0 \\ 0 & 0 & \gamma_1+2\gamma_2 & 0 \\ 0 & 0 & 0 & \gamma_1-2\gamma_2 \end{bmatrix}, \tag{A5a}$$

$$\boldsymbol{H}^{(1)}(\boldsymbol{k}_\parallel)=\frac{\hbar^2}{2m}\begin{bmatrix} 0 & -2\sqrt{3}\gamma_3(k_x-ik_y) & 0 & 0 \\ -2\sqrt{3}\gamma_3(k_x+ik_y) & 0 & 0 & 0 \\ 0 & 0 & 0 & 2\sqrt{3}\gamma_3(k_x-ik_y) \\ 0 & 0 & 2\sqrt{3}\gamma_3(k_x+ik_y) & 0 \end{bmatrix}, \tag{A5b}$$

$$\boldsymbol{H}^{(0)}(\boldsymbol{k}_\parallel)=\frac{\hbar^2}{2m}\begin{bmatrix} (\gamma_1+\gamma_2)k_\parallel^2 & 0 & \sqrt{3}[-\gamma_2(k_x^2-k_y^2)+2i\gamma_3 k_x k_y] & 0 \\ 0 & (\gamma_1-\gamma_2)k_\parallel^2 & 0 & \sqrt{3}[-\gamma_2(k_x^2-k_y^2)+2i\gamma_3 k_x k_y] \\ \sqrt{3}[-\gamma_2(k_x^2-k_y^2)-2i\gamma_3 k_x k_y] & 0 & (\gamma_1-\gamma_2)k_\parallel^2 & 0 \\ 0 & \sqrt{3}[-\gamma_2(k_x^2-k_y^2)-2i\gamma_3 k_x k_y] & 0 & (\gamma_1+\gamma_2)k_\parallel^2 \end{bmatrix}. \tag{A5c}$$

The current density operators is given by

$$\hat{\boldsymbol{J}}_z=\frac{1}{\hbar}(2\boldsymbol{H}^{(2)}k_z+\boldsymbol{H}^{(1)}), \tag{A6}$$

which can be expressed explicitly as

$$\hat{\boldsymbol{J}}_z=\frac{\hbar}{m}\begin{bmatrix} (\gamma_1-2\gamma_2)k_z & -\sqrt{3}\gamma_3(k_x-ik_y) & 0 & 0 \\ -\sqrt{3}\gamma_3(k_x+ik_y) & (\gamma_1+2\gamma_2)k_z & 0 & 0 \\ 0 & 0 & (\gamma_1+2\gamma_2)k_z & \sqrt{3}\gamma_3(k_x-ik_y) \\ 0 & 0 & \sqrt{3}\gamma_3(k_x+ik_y) & (\gamma_1-2\gamma_2)k_z \end{bmatrix}. \tag{A7}$$

*Present address: J. P. Morgan, Akasaka Park Bldg., Akasaka 2-20-5, Minato-ku, Tokyo 107, Japan.
†Also with Department of Physics, National Tsing Hua University, Hsinchu, Taiwan, ROC.

[1] R. Tsu and L. Esaki, Appl. Phys. Lett. **22**, 562 (1973).
[2] E. O. Kane, in *Physics of III-V Compounds*, edited by R. K. Willardson and A. C. Beer, Semiconductors and Semimetals Vol. 1 (Academic, New York, 1966), p. 75.
[3] D. L. Smith and C. Mailhiot, Phys. Rev. B **33**, 8345 (1986).
[4] C. Y. Chao and S. L. Chuang, Phys. Rev. B **43**, 7027 (1991).
[5] D. Y. K. Ko and J. C. Inkson, Phys. Rev. B **38**, 9945 (1988).
[6] D. Z.-Y. Ting, E. T. Yu, and T. C. McGill, Phys. Rev. B **45**, 3583 (1992).
[7] J. N. Schulman and D. Z.-Y. Ting, Phys. Rev. B **45**, 6282 (1992).
[8] T. B. Boykin, J. P. A. van der Wagt, and J. S. Harris, Phys. Rev. B **43**, 4777 (1991).
[9] W. R. Frensley, Rev. Mod. Phys. **62**, 745 (1990).
[10] C. S. Lent and D. J. Kirkner, J. Appl. Phys. **67**, 6353 (1990).
[11] Y. C. Chang, Phys. Rev. B **37**, 8215 (1988).
[12] D. A. Collins, D. Z.-Y. Ting, E. T. Yu, D. H. Chow, J. R. Söderström, and T. C. McGill, J. Cryst. Growth **111**, 664 (1991).
[13] D. Z.-Y. Ting, E. T. Yu, and T. C. McGill, Phys. Rev. B **45**, 3576 (1992).
[14] J. C. Slater and G. F. Koster, Phys. Rev. **94**, 1498 (1954).
[15] D. Z.-Y. Ting and T. C. McGill, Phys. Rev. B **47**, 7281 (1993).
[16] J. M. Luttinger and W. Kohn, Phys. Rev. **97**, 869 (1955).
[17] G. Y. Wu, K.-M. Hung, and C.-J. Chen, Phys. Rev. B **46**, 1521 (1992).
[18] M. Altarelli, Phys. Rev. B **28**, 842 (1983).
[19] J. H. Wilkinson, *The Algebraic Eigenvalue Problem* (Oxford University Press, Oxford, 1965), pp. 633 and 634.
[20] Y. C. Chang and J. N. Schulman, Phys. Rev. B **25**, 3975 (1982).
[21] R. Wessel and M. Altarelli, Phys. Rev. B **39**, 12 802 (1989).
[22] C. Kittel, *Quantum Theory of Solids* (Wiley, New York, 1963).
[23] E. E. Mendez, W. I. Wang, B. Ricco, and L. Esaki, Appl. Phys. Lett. **47**, 415 (1985).
[24] G. L. Bir and G. E. Pikus, *Symmetry and Strain Induced Effects in Semiconductors* (Wiley, New York, 1974).
[25] J. M. Luttinger, Phys. Rev. **102**, 1030 (1956).